ISBN: 978-3-95450-227-1 ISSN: 2673-5490 doi:10.18429/JACoW-IPAC2022-TUPOPT047

PROGRESS REPORT ON POPULATION INVERSION X-RAY LASER OSCILLATOR AT LCLS

A. Halavanau, F. Fuller, R. Robles, R. Margraf, A. Aquila, M. Liang, R. Alonso-Mori,
R. H. Paul, A. A. Lutman, F.-J. Decker, C. Pellegrini
SLAC National Accelerator Laboratory, Stanford University, Menlo Park CA 94025, USA
P. Manwani, N. Majernik, J. B. Rosenzweig
University of California, Los Angeles, CA, 90095, USA
N. Welke, R. Ash, U. Bergmann
University of Wisconsin, Madison, WI, 53706, USA
Š. Krušič, M. Žitnik
Jozef Stefan Institute, Ljubljana, Slovenia
A. Benediktovitch, N. Rohringer
University of Hamburg, CFEL/DESY, Germany

Abstract

We report the progress in the design and construction of a population inversion x-ray laser oscillator (XLO) using LCLS as an x-ray laser pump, being developed by a SLAC, CFEL, University of Hamburg (Germany), University of Wisconsin, Josef Stefan Institute (Slovenia) and UCLA collaboration. In this proceeding, we will present the latest XLO design and numerical simulations substantiated by our first experimental results. In our next experimental step XLO will be tested on the Coherent X-ray Imaging (CXI) end-station at LCLS as a two pass Regenerative Amplifier op-erating at the Copper K_α photon energy of 8048 eV. When built, XLO will generate fully coherent transform limited pulses with about 50 meV FWHM bandwidth. We expect the XLO will pave the way for new user experiments, e.g. in inelastic x-ray scattering, parametric down conversion, quantum science, x-ray interferometry, and external hard x-ray XFEL seeding.

INTRODUCTION

A population inversion X-ray laser oscillator, XLO, pumped by an X-ray FEL like LCLS at SLAC, will provide high intensity, transform limited pulses, opening-up new experimental possibilities in the exploration of atomic and molecular systems at the angstrom/femtosecond space and time scale, interferometry, X-ray quantum science and more. We discuss in this paper several experimental and simulation steps that the XLO collaboration is taking to realize the oscillator. Our present efforts are mainly addressed to a precise determination of the extent of the damage done by the X-ray pump pulse to the gain medium, the development of a solid copper, high speed, gain medium target that would provide fresh copper material to the pumping pulses, repetition of the amplified spontaneous emission (ASE) [1–4] gain measurement with and without external seeding, optical cavity alignment using Si crystals, advanced 3D numerical simulations. In addition, we are working to generate from LCLS the train of pump pulses separated by about 30 ns needed to operate the oscillator. As a first step toward the realization of XLO we will have a two-pulse pump regenerative amplifier.

FAST MOVING SOLID TARGET

In our initial work on XLO we considered using a high-speed jet of a copper nitrate solution as the pump pulse target [5]. Preliminary experiments with the liquid jet have shown that at extreme x-ray power densities the liquid ma-terial undergoes through a process of violent expansion on tens of nanoseconds time scale [6, 7]. This fact prevents the use of simple liquid jet systems in the XLO-like experiments. While an ultra-fast liquid jet is technologically possible, it requires a substantial development and installation effort, and is outside of the scope of our project.

We therefore considered using a fast spinning solid target. There are several advantages of solid w.r.t liquid target. First, a larger, about 10 times, density of copper atoms allows to reduce pump pulse requirements from several mJ, as in the original proposal, to tens of µJ. The reduced pulse intensity is much easier to be achieved at the XFEL, and it drastically reduces the heat load on the cavity in-coupling crystal; see Ref. [1, 5]. The target thickness has been optimized in the state-of-the-art simulation XLO-SIM toolbox that will be described in detail elsewhere [8]. The optimum target width was found to be 25 µm; see Fig. 1. We refer the reader to Refs. [9, 10] for a detailed description of the target assembly and XFEL induced damage.

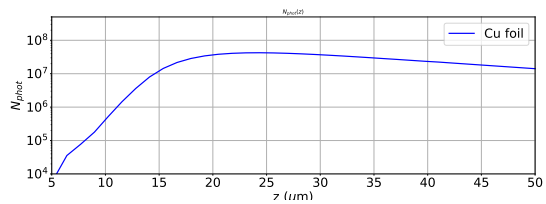

Figure 1: Simulated number of photons after the first pass in the XLO.

ISBN: 978-3-95450-227-1 ISSN: 2673-5490 doi:10.18429/JACoW-IPAC2022-TUPOPT047

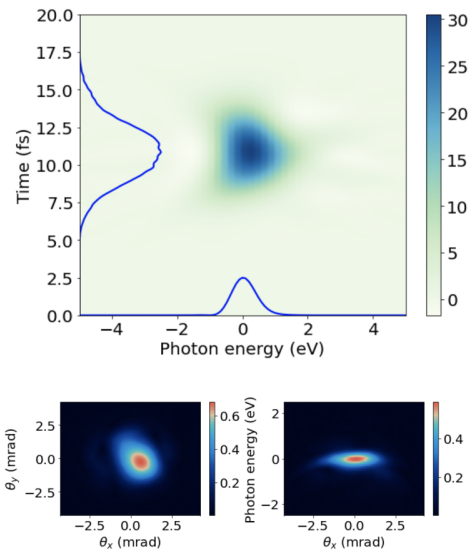

Figure 2: Simulated x-ray radiation profile at the exit of the copper target: Wigner's time-frequency distribution (top) and angular and spectral-angular distributions (bottom) after the first pump pulse.

X-RAY CAVITY DESIGN

At the exit of the gain medium, the x-ray radiation may possess certain degree of coherence, as it can be seen in Fig. 2. However, it should be noted, that due to the sponta-neous nature of the initial XLO pulse, similar to SASE of the electron beam, intensity fluctuations may occur. Therefore, the purpose of Bragg crystal cavity is not only to return the radiation but to also drastically improve the coherence.

We performed the initial cavity design investigation as-suming flat perfect Silicon crystals and ideal Be compound refractive lenses (CRL). The cavity layout is presented in Fig. 3. In brief, four flat perfect Si (4,4,4) crystals (C1-C4) make up a cavity, recirculating the x-ray beam in a clock-wise direction. Crystals C2 and C3 have adjustable positions to enable cavity length tunability, from 8500 mm to 10 500 mm. The cavity radiation is refocused with a CRL onto the target foil. XLO cavity crystals have been procured from Sarton Works (Japan) in a form of 1 inch cubes (C1-C3) and 50 µm membranes (C4). We characterized the crystal reflectivity using in-house rocking curve imaging (RCI) setup at SSRL beamline 10-2; see Ref. [11], and compared it with the ana-lytical formula for crystal reflectivity. We found the crystals to be very close to perfect, as it is expected from highest grade Silicon; see Fig. 4. The dispersive nature of the Bragg reflection results in spectral-angular acceptance, that can be described in a form of DuMond diagram; see Fig. 5. X-ray propagation through the thin Silicon membrane (C4) is in-vestigated using the adapted multi-slice method, recently presented in Ref. [12].

In addition, a significant collimation is expected through the CRL element.

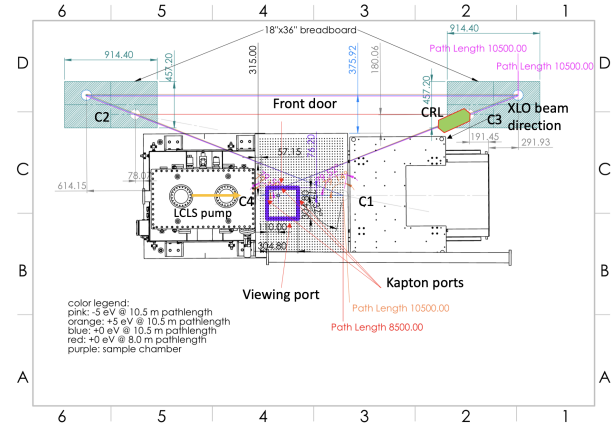

Figure 3: Top view of the first XLO experiment in the CXI hutch at LCLS.

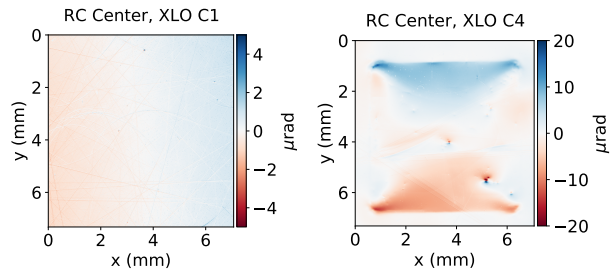

Figure 4: Rocking curve maps of the XLO crystal 1 (thick Si block, left) and crystal 4 (thin membrane, right).

PLANNED EXPERIMENTAL PROGRAM

The initial demonstration of XLO will be done with Si (444) crystals, in back-scattering bow-tie geometry. The LCLS-II HXR undulator will be tuned to provide 9 keV pump pulses, with the first 3-4 undulators will be used for seeding with 8 keV. We note that due to the Lorentzian nature of the atomic lines, it is possible to seed the stimulated emission process in Copper at K_α line, even 10 eV away from it in energy. The latter fact allows for the most of the "seeding" SASE pulse to enhance the probability of emission, while not being recirculated in the cavity [13].

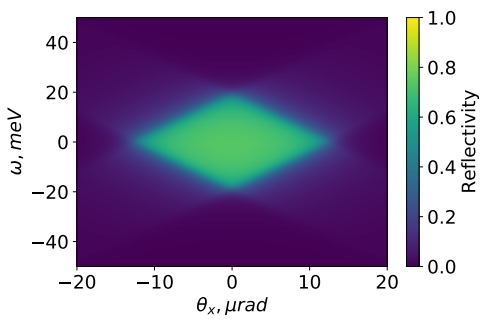

Figure 5: DuMond diagram of the ideal bow-tie x-ray Si (4,4,4) cavity as shown in Fig. 3.

ISBN: 978-3-95450-227-1 ISSN: 2673-5490 doi:10.18429/JACoW-IPAC2022-TUPOPT047

In the upcoming round of XLO experiments we will first focus on the demonstration of target replenishment and cavity performance. We will measure the target damage as a function of pump intensity, and determine the minimum rotation speed needed for target replenishment. After that, we will proceed with establishing the cavity reflections. The XLO beam will be sent onto C1, and the crystal will be rocked around the theta axis to find Bragg reflection. The reflection intensity will be optimized with a highly sensitive PIPS diode at the C2 location, and the exercise will be repeated for C2 and C3. Finally, after the alignment of crystal C4 will be done by placing the diode behind it and rocking it to minimize the signal on the diode. In order to continue the cavity alignment, namely making sure the reflections stay in plane, we will introduce an intra-cavity diagnostics element, thin Si membrane, followed by the fast photodiode. Using this diagnostics we can ensure multiple cavity roundtrips.

After the cavity studies, we will proceed with generating two consequtive XLO pulses ~ 30 ns apart. We will use the LCLS multi-bunch capabilities [14]. The two- and multi-bunch performance of the LCLS copper linac has been recently improved by introducing two stripline-style kickers in early in the machine [15].

SUMMARY

XLO, when built, will become an additional highly coherent hard x-ray source at LCLS, enabling many potential new experiments. A vibrant program is underway at LCLS to perform first cavity experiments in the near future.

ACKNOWLEDGEMENTS

This work is supported by the U.S. Department of Energy Contract No. DE-AC02-76SF00515.

REFERENCES

[1] H. Yoneda *et al.*, "Atomic inner-shell laser at 1.5-Angstrom wavelength pumped by an x-ray free-electron laser", *Nature*, vol. 524, pp. 446–449, 2015. doi:10.1038/nature14894

[2] N. Rohringer *et al.*, "Atomic inner-shell x-ray laser at 1.46 nanometres pumped by an x-ray free-electron laser", *Nature*, vol. 481, pp. 488–491, 2012. doi:10.1038/nature10721

[3] T. Kroll *et al.*, "Stimulated x-ray emission spectroscopy in transition metal complexes", *Phys. Rev. Lett.*, vol. 120, p. 133203, 2018. doi:10.1103/PhysRevLett.120.133203

[4] T. Kroll *et al.*, "Observation of seeded mn Kβ stimulated x-ray emission using two-color x-ray free-electron laser pulses", *Phys. Rev. Lett.*, vol. 125, p. 037404, 2020. doi:10.1103/PhysRevLett.125.037404

[5] A. Halavanau *et al.*, "Population inversion x-ray laser oscil-lator", *Proceedings of the National Academy of Sciences*, vol. 117, no. 27, pp. 15511–15516, 2020.

[6] A. Halavanau *et al.*, "Progress Report on Population Inversion-Based X-Ray Laser Oscillator", in *Proc. IPAC'21*, Campinas, Brazil, May 2021, pp. 373–375. doi:10.18429/JACoW-IPAC2021-MOPAB100

[7] M. Yadav *et al.*, "Optimization of the Gain Medium Delivery System for an X-Ray Laser Oscillator", in *Proc. IPAC'21*, Campinas, Brazil, May 2021, pp. 524–527. doi:10.18429/JACoW-IPAC2021-MOPAB150

[8] A. Benediktovitch *et al.*, In preparation.

[9] N. Majernik *et al.*, "Foiled Again: Solid-State Sample De-livery for High Repetition Rate XFELs", presented at the IPAC'22, Bangkok, Thailand, Jun. 2022, paper THPOTK053, this conference.

[10] P. Manwani *et al.*, "Modelling of X-Ray Volume Excitation of the XLO Gain Medium", presented at the IPAC'22, Bangkok, Thailand, Jun. 2022, paper TUPOPT034, this conference.

[11] A. Halavanau *et al.*, "Rocking Curve Imaging Experi-ment at SSRL 10-2 Beamline", in *Proc. IPAC'21*, Camp-inas, Brazil, May 2021, pp. 357–360. doi:10.18429/JACoW-IPAC2021-MOPAB096

[12] J. Krzywinski and A. Halavanau. "Time-dependent dynami-cal Bragg diffraction in crystals by beam propagation method (bpm)", *arXiv preprint*, 2022. doi:10.48550/arXiv.2201.08500

[13] A. Halavanau, M. Doyle, *et. al*, "Observed intensity limits for seeded stimulated x-ray emission at the Mn Kα wavelength", in progress.

[14] F.-J. Decker *et al.*, "Tunable x-ray free electron laser multi-pulses with nanosecond separation", *Sci-entific Reports*, vol. 12, p. 3253, 2022. doi:10.1038/s41598-022-06754-y

[15] A. Halavanau *et al.*, "LCLS Multi-Bunch Improvement Plan: First Results", presented at the IPAC'22, Bangkok, Thailand, Jun. 2022, paper TUPOPT037, this conference.